Journal of Microelectronics and Electronic Packaging (2013) **10**, 109-115

ISSN: 1551-4897

Aerosol Jet Printing of Two Component Thick Film Resistors on LTCC

K. Swiecinski, M. Ihle, R. Jurk, E. Dietzen, U. Partsch, and M. Eberstein*

Abstract—**Aerosol jet printing is a rather new technology for the deposition of thick film structures offering high line and space resolution. This method offers high potential for miniaturization for thick film structures. The advantages of this technology could be shown with inks carrying a single solid powder (e.g., silver, platinum, ceramic, or glass powder). One of the challenges in printing solid powder mixtures is the differences in the aerodynamic properties of different powders. Those differences result in changes of the mixing ratio within the aerosol jet and therefore poor reproducibility in the finished film.**

In this work, thick film resistors consisting of RuO_2 with particle size <1 μm as the conducting phase and different glass powders with particle size around 1 μm as the isolating phase were investigated. One glass had a density rather close to RuO_2, the other glass significantly lower. Inks were made from RuO_2/glass powder mixtures, a solvent, and organic additives. After manufacturing, the inks are printed on LTCC and the microstructures of the dried and the fired films were visualized by FIB preparation and SEM. The resistances as well as the temperature coefficients of the resistors were measured and compared with resistor films with an identical solid composition manufactured by conventional screen printing. The results of the obtained resistors are presented and discussed in terms of powder properties, ink dispersion, and printing parameters.

Keywords—**Thick film resistor, glass sintering, aerosol printing, miniaturization**

Introduction

Ceramic packaging has been successfully used for the fabrication of microelectronic devices such as chip carriers, controllers, and microsystems featuring integrated channels and cavities for fluids, mechanical, and even chemical sensors [1]. Facing new technologies such as green energy or electromobility, a continuous growing demand for temperature stable and robust ceramic electronic devices is expected. In addition, the degree of functional integration is expected to rise, and as a result, the geometrical dimensions of such devices should be minimized. These requirements were fulfilled over many years by continuous introduction of novel materials, device design, and fabrication technologies. The miniaturization of thick film resistors has been realized by the addition of sophisticated structuring techniques to commercial thick films obtained from the standard screen print process. Lateral dimensions of 50 × 50 μm^2 to 50 × 70 μm^2 were attained by applying photolithography to photoimageable pastes [2, 3], and dimensions of 30 × 30 μm^2 were obtained by laser shaping [4]. In addition, a stamp print of spin coated inks in a fine line pattern was introduced [5]. A very young technology for the maskless, economic deposition of high resolution thick film metallization is aerosol jet printing. Hereby, a low viscous suspension carrying the metallization particles (ink) is transferred by pneumatic atomization, labeled (1) in Fig. 1, into an aerosol (9). Furthermore, this aerosol is compacted in the virtual impactor (3) and led to the nozzle in the deposition head (4) and focused on the substrate (5) to give lines and spaces of only 10 microns in width (Fig. 1) [6]. This is much lower than screen print (50-80 microns) or ink jet print (>40 microns) and features a huge miniaturization potential for maskless direct printed thick film structures. In addition, the focus length of the aerosol stream amounts to 1-5 mm, which easily enables printing over edges or tubes.

Nevertheless, only single-solid-containing inks featuring silver or gold nano particles were deposited and fired to give fine line conductors, as of the current time [6]. However, resistor layers typically consist of an isolating glass matrix phase through which conducting paths are formed by a crystalline phase (e.g., RuO_2 or AgPd). After mixing, the conducting particles are located between the glass particles. During sintering, the glass particles densify to a thoroughly connected matrix through which the conducting particles form percolation paths, making up the sheet resistance [7] (Fig. 2).

The processing of mixtures of different materials having different particle sizes through an aerosol jet stream has not been reported so far. The aim of this work is to investigate the processability of two resistor powder mixtures via aerosol jet print. The focus of this study is the influence of the glass properties on the ink dispersion, deposition properties, layer formation and the resulting film properties.

Experimental

A. Resistor Powder

A simple and common resistor powder recipe has 20 vol.% of a fine RuO_2 powder (703-02L, Heraeus, Hanau) with a submicron particle distribution (see Fig. 3) as the conducting phase and 80 vol.% of a coarser dispersed isolating glass phase. Sedimentation and clogging of ink droplets in tubes of the aerosol jet printer result in a limitation of the droplet size to

The manuscript was received on June 20, 2013; revision received on August 22, 2013; accepted on August 22, 2013

Fraunhofer Institute for Ceramic Technologies and Systems, Winterbergstr. 28 01277, Dresden, Germany

*Corresponding author; email: markus.eberstein@ikts.fraunhofer.de

doi:10.4071/imaps.384

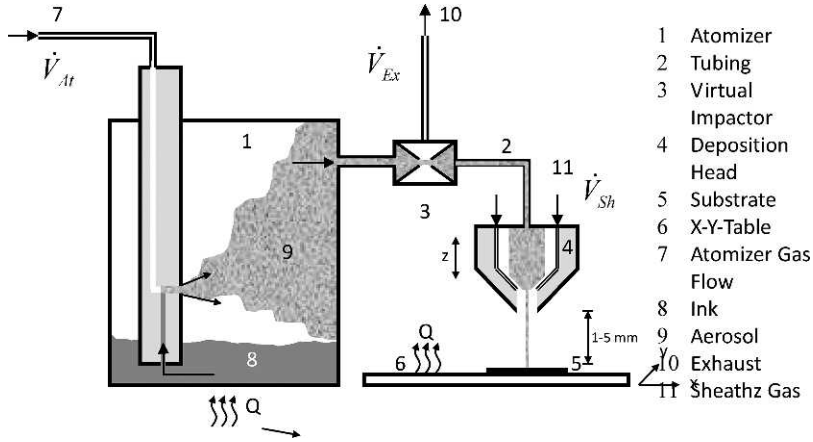

Fig. 1. Scheme of aerosol jet process.

5 μm [13]. This limitation forces the particle size of inorganic powders to be even smaller. For the isolating matrix, two glasses having different composition and density according to Table I were used.

Glass 1 contains 65 wt.% PbO with a density of 3.90 g/cm^3. Glass 2 is lead-free and shows a transformation temperature (T_g) in the same range as Glass 1 but only about half of its density. The glasses were melted in an electrical furnace (Carbolite RHF1600) and fritted into water. The glass frits obtained were milled in a planetary ball mill and an attritor (Netzsch) to very similar particle size distributions of around 1 μm as shown in Fig. 3. The thermal expansion coefficient (TEC) and transformation temperatures of the glasses were determined by a standard dilatometer.

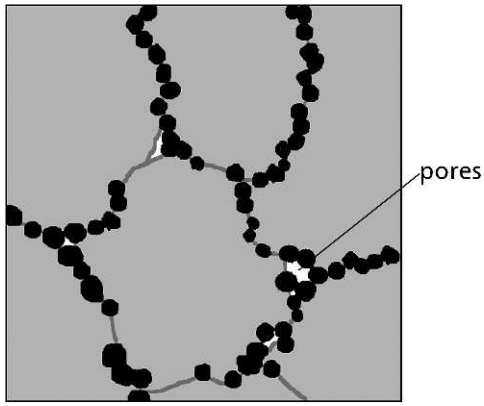

Fig. 2. Principal scheme of a resistor layer after sintering. The glass particles form a thoroughly connected isolating matrix through which the conducting particles form percolation paths making up the sheet resistance [7].

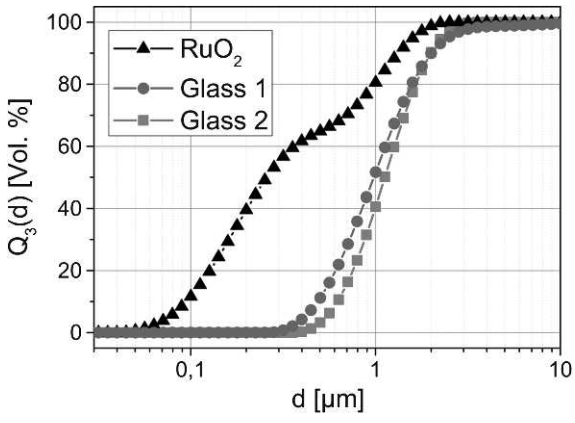

Fig. 3. Particle size distributions of the RuO_2 powder, Glass 1, and Glass 2 used in this work.

B. Ink and Paste Preparation

Each powder mixture was divided into two parts. The first part was used to manufacture an ink suited to aerosol jet printing. The solvent in the ink was N-methyl-pyrolidone (Sigma Aldrich); the polymer ethylcellulose (46080, Sigma Aldrich) was used to set the viscosity at 100 mPa·s (at 25°C, 100 s^{-1}, Haake Mars), and tenside was used as a dispersant. The second part of each powder was used to fabricate a conventional screen print paste. Here, terpineole served as a solvent, whereas ethycellulose was also used as a polymer.

C. Printing and Firing

Fired LTCC DP951 was used as the substrate ceramic. The conductor paste was printed with a 200 mesh screen, and leveled at room temperature for 10 min by using a standard screen printer (Ekra Mikrotronic II). The printed structures were dried for 15 min at 150°C and fired at 850°C in an air atmosphere in a belt furnace with a dwell time of 10 min and total cycle time of 60 min.

The test pattern for all printed inks and pastes is shown in Fig. 4. This test pattern features 16 resistors after printing three lines of resistor paste perpendicular to the contacting

Table I
Selected Glass Compositions and Some Thermal Data of Glass 1 and Glass 2

Glass	Glass 1	Glass 2
ρ [g/cm^3]	3.90	2.20
T_g [°C]	513	495
TEC [ppm K^{-1}]	8.4	2.8
PbO content	Yes	No

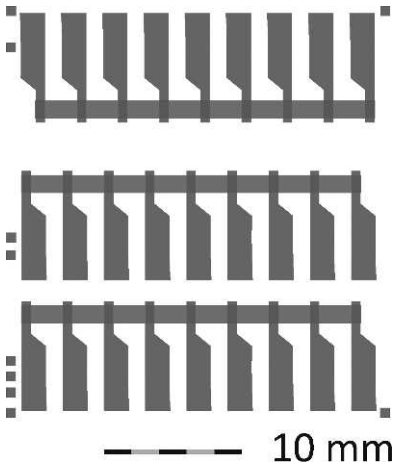

Fig. 4. Test pattern for all printed inks and pastes. Green: silver contacts (printed and fired first), red: resistor films (postfired). Each substrate features 24 resistors, 2 × 1 mm in size.

pads. The film properties of the screen printed layer of each powder were used as a reference for comparison with the film properties obtained by aerosol jet print. The printing speed of the aerosol jet printer is about 3 mm/s. Print duration for a whole resistor test pattern according to Fig. 4 depends on volume stream and focus settings, and typically amounts to 2 min. The viscosities and selected processing data of the tested inks in aerosol printing are given in Table II.

The contacting pads are obtained by screen printing and firing an Ag-Pd-paste. The test pattern geometry was matched to an automated measuring head detecting the resistance, R, and the temperature coefficient of the resistance (TCR).

D. Characterization

The sinter densification of the layer was observed by an in situ resistance measurement. The printed and dried pattern was contacted by gold wires and fired in a tube furnace at a rate of 10 K/min. The cross sections of aerosol jet printed and dried films were prepared by focused ion beam (FIB) and observed in the FESEM (Crossbeam NIVISION 40). The film porosity and the volume amounts of glass and RuO_2 in the films were examined by FESEM image analysis.

Results

A. Dispersion and Printability

In Table II, viscosities of selected inks are specified. The aerosol jet printability of ink I024 was satisfying after little tuning of the organics recipe. In contrast, the lead-free Glass 2 gives significant changed ink properties. The same surfactant and same amount of ethylcellulose as in ink I024 results in a viscosity of only 40 mPa·s, presumably due to the changed dispersion quality. The aerosol jet print typically features a risk of ink deposition in the transport tubes due to the precipitation and subsequent coagulation of aerosol droplets. A well-tuned ink does not show such effects until a large number of process hours have passed. In the investigation, the high density ink I024 showed minimal precipitation and coagulation tendency, whereas for the low density ink I029, the effect was more pronounced. By changing the polymer to polyvinylpyrrolidone (PVP, MW: 10,000), the viscosity was increased and a printability of this ink was attained. However, the total amount of the polymer in the ink I029 containing the low density Glass 2 was 10 wt.%, whereas it amounted to only 2 wt.% in the ink I024 containing the high density Glass 1.

Table II
Viscosities and Volume Stream Data According to Fig. 1 of the Aerosol Inks Tested

Ink	I024	I029
Viscosity [mPa·s]	100	95
$\dot{V}_{Sh}$[cm^3·min^{-1}]	50	50
$\dot{V}_{At}$[cm^3·min^{-1}]	950-1,000	470-530
$\dot{V}_{Ex}$[cm^3·min^{-1}]	930-970	450-500

Selected print parameters of the inks I024 und I029 are also listed in Table II. The major difference in the process parameters is the atomizer flow rate $\dot{V}_{At}$. For I024 (high density Glass 1) this volume stream had to be set to 950-1,000 cm^3/min, whereas for I029 (low density Glass 2) it needed only 470-530 cm^3/min to generate an aerosol density sufficient for printing.

B. Properties of the Dried Films

Fig. 5 depicts cross sections of the printed and dried films of the inks I024 and I029. Both films show homogenous distribution of glass particles (middle gray); RuO_2 particles (bright); polymer residuals (dark gray); and pores (black). In the microstructure of I024, the dispersion of RuO_2 particles in the glass particle matrix is more homogeneous, whereas in the microstructure of I029 tendency of agglomeration of RuO_2 particles can be observed. By means of image analysis, the volume amounts of glass and RuO_2 in the deposited films of I024 and I029 were estimated and are specified in Table III.

In both films, the glass to RuO_2 ratio is decreased relative to the respective ink. The film of the ink I024 contains approximately 22% RuO_2 and the film formed by the ink I029 contains 26% RuO_2. The particle size distributions of the deposited films were examined by manual counting in the images presented by Fig. 5. The results are shown in Fig. 6 and Fig. 7 and point to a pronounced grading effect of the aerosol jet process. From ink I024 containing the high density Glass 1, only particles smaller than 1 μm were deposited on the substrate; whereas, in the case of ink I029 containing the low density Glass 2, only particles smaller than 0.8 μm were found. Due to the limited accuracy of the counting procedure, both values may be regarded as similar, around 1 μm. The initial particle size distribution (PSD) of RuO_2 and glass in each ink is plotted in Fig. 6 and in Fig. 7. Because glass powder and RuO_2 powder have different fractions in the range below the separation size, the grading leads to a shift toward a higher RuO_2 to glass ratio. The shift observed for ink I024 containing the high density Glass 1 is rather slight, whereas the shift observed for ink I029 containing the low density Glass 2 is more pronounced (Table III).

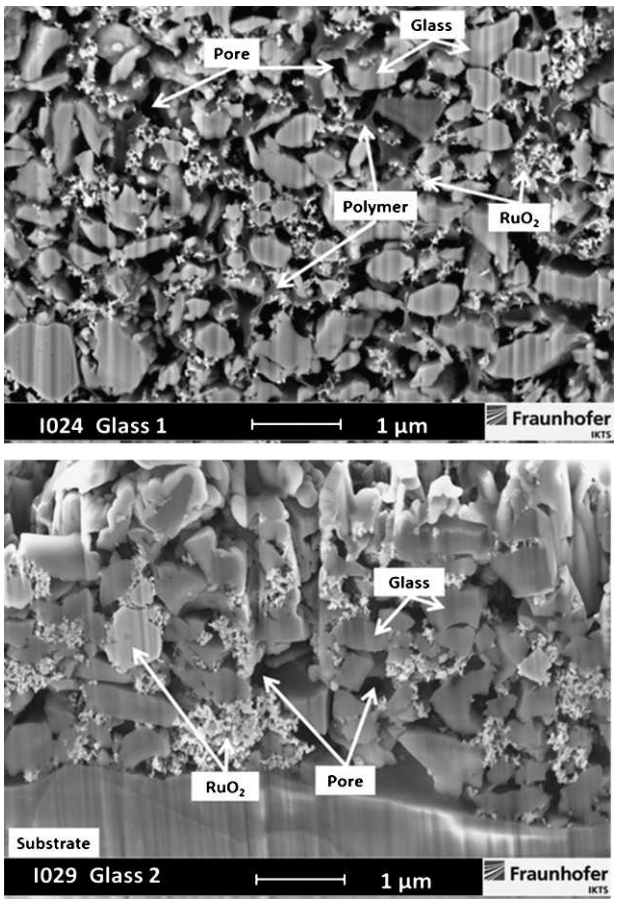

Fig. 5. Cross sections of the microstructures printed and dried films of the inks I024 and I029, obtained by FIB preparation. Glass particles: medium gray; RuO_2 particles: bright; polymer residuals: dark gray; pores: black.

Table III
Volume Amounts of Glass and RuO_2 in the Ink and in the Deposited Films of I024 and I029 as Estimated by Image Analysis

	Ink	I024	I029
Glass [vol.%]	80	78	74
RuO_2 [vol.%]	20	22	26

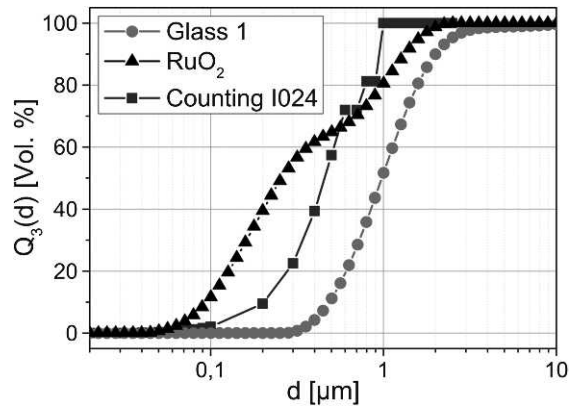

Fig. 6. PSD of the inorganic solids in the deposited and dried film of ink I024, obtained by image analysis. The initial PSD of RuO_2 and glass for each ink is plotted for comparison.

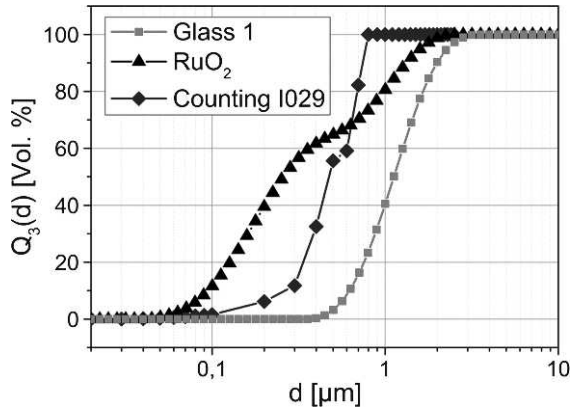

Fig. 7. PSD of the inorganic solids in the deposited and dried film of ink I029, obtained by image analysis. The initial PSD of RuO_2 and glass for each ink is plotted for comparison.

C. Sintering Behavior

The in situ measurement of the resistance is a valuable method for the observation of densification and microstructural effects during firing of thick film resistors [8]. The resistance of the deposited and dried ink I024 as a function of temperature is presented in Fig. 8 (blue line). For comparison, a similar measurement was performed using the screen print paste R801 containing the same solids as the ink (Fig. 8, red line). At about 550°C, the resistance of the aerosol jet powder starts to decrease and shows a sharp drop to 4×10^3 at 610°C, indicating densification of the glass powder and formation of conducting paths by percolating RuO_2 particles. After passing this temperature, a little rise of the resistance with a first slight maximum at 650°C and a second maximum at 850°C are observed, along with the dwell temperature of the measuring cycle. The first slight maximum is attributed to the occurrence of two counteracting effects. First, a crystalline phase occurs at 650°C and pushes some percolating RuO_2 particles away from each other, creating a decreasing number of percolation paths. Second, a further rise of the sintering temperature lowers the viscosity of the glass phase, which promotes sinter densification [9] forming new percolation paths. A final increase of the resistance at 850°C is regarded to result from a further amount of crystallization during the dwell time.

A polished cross section of the fired layer is shown in Fig. 9. The glass matrix appears smooth in middle gray color. The bright little submicron particles are RuO_2. A third phase can be recognized as round particles, with a size of about one micron and dark gray color. This phase could be identified as SiO_2 crystals (EDX data not shown), which obviously crystallized after film densification. Unfortunately, the crystal modification quartz or cristobalite could not be identified in this investigation.

The SiO_2 crystals have at least two effects on the film, namely, the decrease of the perlocation degree of the conducting RuO_2 particles and an increase of the temperature coefficient of expansion (TCE) of the layer. In total, this results in a positive

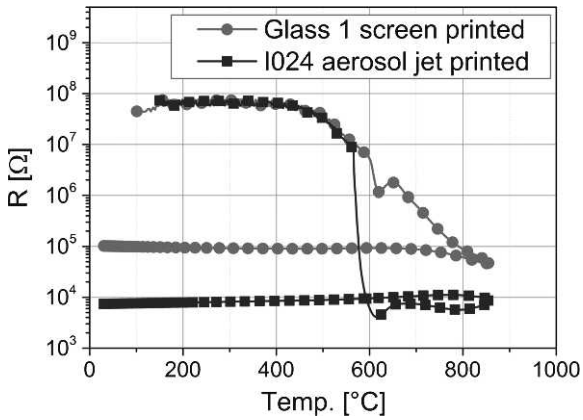

Fig. 8. Resistance of deposited and dried films manufactured by aerosol jet print of the ink I024 (red) as well as screen print of a paste containing the same solids (blue) as a function of temperature.

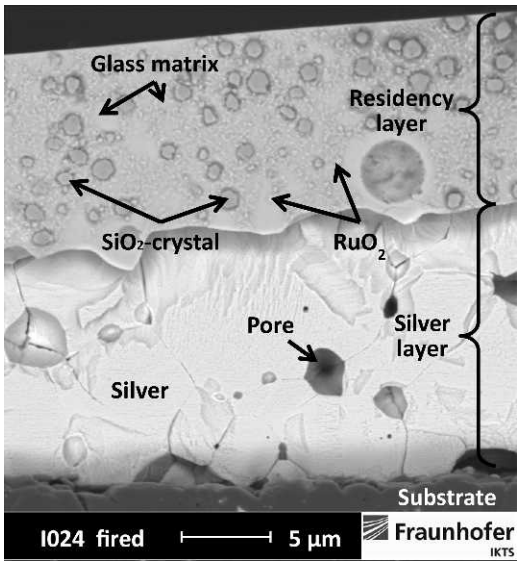

Fig. 9. Polished cross section of aerosol jet printed resistor film of I024 after firing at 850°C at the overlap to the Ag-Pd contacts. Phases are indicated by labels.

temperature coefficient of resistance (TCR). This becomes evident during the cooling down phase of the film (Fig. 8), where the resistance is decreased to approximately $8 \times 10^3\ \Omega$.

The effect of the crystallization of SiO_2 from the glass is more pronounced in the sintering behavior of the screen printed film. The PSD has a strong influence on the densification temperature of a glass ceramic powder [10]. In this investigation, the screen printed powder densifies at a 50 K higher temperature. This results in the fact that the crystallization of the film occurs in an early stage of powder densification and a decrease of the overall sintering rate.

The final resistance of this film of about $4 \times 10^5\ \Omega$ is attained not before 850°C and amounts to one order of magnitude higher than that of the aerosol jet printed film. This can be caused by the higher amount of RuO_2 in the aerosol printed layer and/or shifted crystal morphology in the film microstructure. Those effects might also be related to the negative TCR found during the cooling down phase of the film.

Table IV
Properties of the Fired Resistors Obtained from the Pastes R801 and R802 (Screen Printed) and from the inks I024 and I029 (Aerosol Jet Printed)

Paste/ink	R801	I024	R802	I029
Glass	Glass 1		Glass 2	
T_{Sinter} [°C]	610		850	
R_{sq} [Ω/sq]	1.35×10^6	2.25×10^3	25	—
TCR [ppm/K]	−400	620	1270	—
Printed layer quality	OK	OK	OK	Cracks

D. Properties of the Fired Films

Table IV specifies properties of the aerosol jet printed and screen printed resistor films manufactured using powders of RuO_2 and Glass 1 and Glass 2, respectively. If the films of the aerosol jet ink I024 are fired at 610°C instead at 850°C, the glass crystallization can be avoided. Values for this firing temperature are given in Table IV for comparison. The observed difference between aerosol jet printed and screen printed resistor films at 610°C can be explained by grading of the powder during the aerosol jet print. A finer glass powder leads to more conduction paths and therefore a lower film resistance for the aerosol jet printed film of the I024 compared with R801 [11]. The larger number of conduction paths may also influence the TCR, which is 620 ppm/K for I024 and is −400 ppm/K for R801. The overall current in thick film resistors is the sum of conducting effects (e.g., in an RuO_2 particle) having positive TCR and semiconducting effects (e.g., RuO_2 particle/thin glass/RuO_2 particle) having negative TCR. The positive TCR value for the I024 is seen to be caused by a higher number of conducting paths, whereas higher glass amounts in the R801 may lead to a negative value. Using the low density Glass 2, in the framework of this investigation, no sufficient film quality could be attained using aerosol jet print.

For the aerosol jet printed films of ink I024, a study of reproducibility was done by printing resistors in different thicknesses on a number of substrates. The prints were carried on different days (not indicated in the figure). The result is shown in Fig. 10. The resistance, as well as the TCR values of films produced by aerosol jet printing of ink I024, in dependence of film thickness and printing time, show negligible deviations.

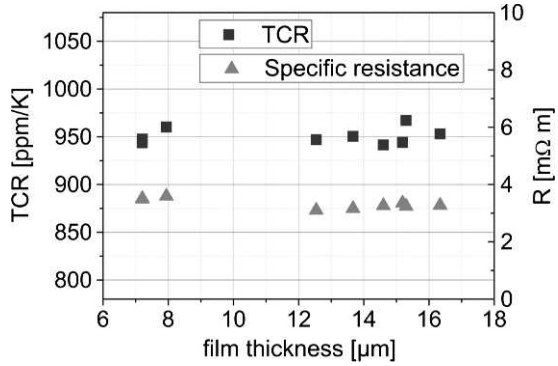

Fig. 10. Resistance and TCR values of films produced by aerosol jet print of the ink I024 dependent on film thickness.

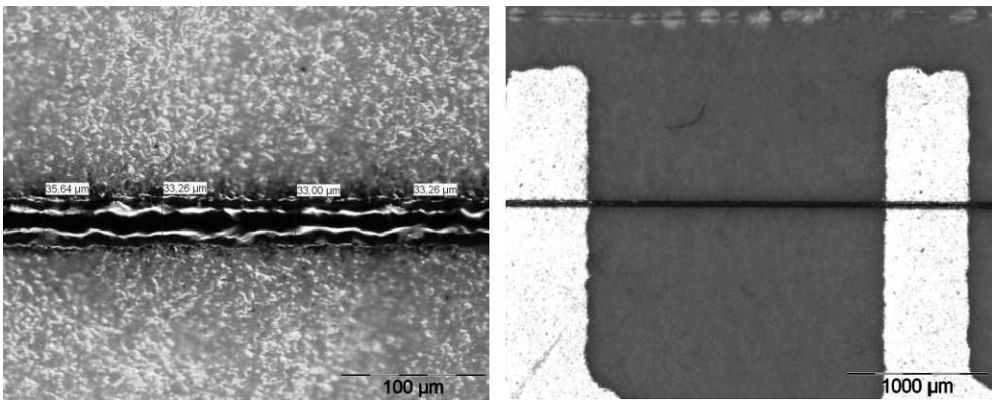

Fig. 11. Example of a fine line resistor film manufactured using ink I024. Blue: LTCC substrate; bright: AgPd contacts; black: resistor film.

For evaluation of the miniaturization potential of the aerosol jet technology regarding resistor thick films, a fine line printing test was performed. After tuning the print parameters carefully, a layer with a line width of 30 µm, a height of 11 µm (10 times print), and a length of 2.1 mm could be deposited. The total print duration at a speed of 3 mm/s was lower than 10 s. An image of the resulting film is shown in Fig. 11. The sheet resistance of this line amounts to 1.7 k/sq, the absolute resistance to 100 k, and the TCR to 500 ppm/K.

Discussion

Compared with common screen print technology, aerosol jet print technology puts additional requirements on the powder suspension used, namely a sufficient dispersion and a particle size in the submicron range. An influence of the glass phases used in this investigation was observed in (i) the dispersion quality and printability of the ink, (ii) the grading behavior during the aerosol jet print, and (iii) in the sintering behavior of the deposited films.

For a conventional resistor architecture, the isolation glass powder must have a coarser PSD than the RuO_2, on the one hand, but will be graded at around one micron in the print process, on the other hand. For this reason, the process window for the glass particle size is narrow in an aerosol print ink. Thus, with respect to the fact that usual glass powder conditioning and milling in the nanoscale is challenging, some grading may often occur and must be included in the powder formulation.

The glass powder composition has an important influence on the dispersal and on the printability of the suspension. In this investigation, the high density Glass 1 was relatively easy to process, whereas the low density Glass 2 was very challenging to disperse and print. However, aside from the glass density, the surface potentials of the two glass powders in the solvent are expected to be different due to the differences in the chemical compositions; for example, Glass 1 contains 65 wt.% PbO, whereas Glass 2 is PbO-free. Therefore, the adsorption with specific surfactants can be different, which will also influence the dispersion quality. Further studies on resistor inks for aerosol printing should give attention to these phenomena.

The glass density had a strong influence on the atomizer flow rate. As the viscosities of the inks are comparable, this fact points to the impact of ink density, which is tightly linked to the glass density. The aerosol densities in the atomizer were not measured but should be approximately equal to each other, because the deposition rates obtained with both inks are found at the same level (Table I).

The grading effect of the aerosol jet process had a large impact on the total particle size and volume ratio of RuO_2 to glass in the deposited films. Due to the essential impact of these parameters for a resistor recipe, the grading effect is a major issue for future developments. In this investigation, the grading leads to a shift toward higher values of the RuO_2 to glass ratio. A higher RuO_2 fraction should result in a lower sheet resistance of the fired aerosol printed thick film, compared with an ungraded screen printed film. This was confirmed by the sheet resistances of those films measured (Table IV). Finally, because decreasing particle size of a glass powder causes a shift of the sinter onset to a lower temperature, the grading effect also has an impact on the film sintering properties. Moreover, in an aerosol jet resistor ink, it is clear that the glass crystallization behavior is influenced by the particle size [12].

The long-term stability of the aerosol jet printed resistors have not been tested in the framework of the investigation.

Conclusions

In this work, the deposition of common conventional thick film resistor powder recipes by aerosol jet printing was investigated. The inks consist of RuO_2 with particle size < 1 µm as the conducting phase and two different glass powders as the isolating phase dispersed in a solvent with organic additives. Glass 1 has a high density, whereas Glass 2 is significantly lighter. The inks were printed on LTCC and the microstructures of the dried and the fired films were visualized. Sintering was observed by online resistor measurements. The resistances as well as the temperature coefficients of the resistors were determined and compared with resistor films manufactured by conventional screen printing. This work has shown that the glass phase has great influence on (i) the dispersion quality of the ink, (ii) the grading behavior during the aerosol jet print, and (iii) in the sintering characteristics of the deposited films. The aerosol jet process shows a grading effect on the total particle size and changes in the volume ratio of RuO_2 to glass in the deposited films. This effect is a main issue and has to

be addressed in appropriate future developments. Utilization of the high density Glass 1, dispersal, printability, and sinter parameters could be set to produce resistor layers with high reproducibility in sheet resistance and temperature coefficient. The miniaturization power of aerosol jet print for thick film resistors was demonstrated by the realization of a resistor film of only 30 μm in width.

References

[1] D.L. Wilcox and M. Oliver, "LTCC, an interconnect technology morphing into a strategic microsystem integration technology," Proceedings of Advanced Technology Workshop on Ceramic Applications for Microwave and Photonic Packaging, IMAPS, Providence, RI, 2002.

[2] J. Minalgiene and V. Baltrusaitis, "Photoimageable thick film implementation of very high density ceramics technology products," Proceedings of the 39th IMAPS Nordic Annual Conference, Stockholm, pp. 233-242, 2002.

[3] A. Dziedic, L. Rebenklau, L.J. Golonka, and K.-J. Wolter, "Fodel microresistors; Processing and basic electrical properties," *Microelectronics and Reliability*, Vol. 43, No. 3, pp. 377-383, 2003.

[4] D. Nowak, E. Mis, A. Dziedic, and J. Kita; "Fabrication and electrical properties of laser-shaped thick-film and LTCC microresistors," *Microelectronics and Reliability*, Vol. 49, No. 6, pp. 600-606, 2009.

[5] C. Lakeman and P. Fleig, "High resolution integration of passives using micro-contact printing (mCP)," *Microelectronics International*, Vol. 20, No. 1, pp. 52-55, 2003.

[6] M. Ihle, U. Partsch, S. Mosch, and A. Golberg, "Aerosol printing of high resolution films for LTCC-multilayer components," *Journal of Microelectronics and Electronic Packaging*, Vol. 9, No. 3, pp. 133-137, 2012.

[7] R. Schmidt, C. Kretzschmar, and M. Eberstein, "Influence of film thicknesses on the electrical properties of RuO_2-thick film resistors on aluminium nitride ceramics (AlN)," Proceedings of Bringing Together the Entire Microelectronics Supply Chain, IMAPS, 2011.

[8] T. Nakano and T. Yamaguchi, "Studies on sintering of RuO_2-glass TFRs by in-situ resistance measurement," *International Journal of Microcircuits and Electronic Packaging*, Vol. 16, No. 1, pp. 61-70, 1993.

[9] M. Eberstein, T. Rabe, and W.A. Schiller, "Influences of the glass phase on densification, microstructure, and properties of low-temperature co-fired ceramics," *International Journal of Applied Ceramic Technology,* Vol. 3, No. 6, pp. 428-436, 2007.

[10] R. Müller, S. Reinsch, M. Eberstein, J. Deubener, A. Thiel, and W.A. Schiller, "Effects of dispersed Al_2O_3 particles on sintering of LTCC," *Advanced Materials Research*, Vol. 39-40, pp. 375-380, 2008.

[11] S. Dietrich, C. Kretzschmar, U. Partsch, and L. Rebenklau, "Reliability and effective signal-to-noise ratio of RuO_2-based thick film strain gauges: The effect of conductive and glass particle size," Proceedings of the 32nd International Spring Seminar on Electronics Technology, ISSE, pp. 13-17, 2009.

[12] W. Kingery and M.D. Narasimhan, "Densification during sintering in the presence of a liquid phase. II. Experimental," *Journal of Applied Physics*, Vol. 30, No. 3, pp. 301-310, 1959.

[13] M. Hedges, "3D large area printed and organic electronics via the aerosol jet process," Proceedings of the International Conference and Exhibition for the Organics and Printed Electronics Industry, LOPE-C, Messegelände Frankfurt, 2010.